THE JOURNAL OF PHYSICAL CHEMISTRY B

ARTICLE

pubs.acs.org/JPCB

High-Pressure Investigations of a Ferroelectric Liquid Crystal Exhibiting a Trend Reversal in the Thermal Variation of Polarization

Prasad N. Bapat,[†] D. S. Shankar Rao,[†] S. Krishna Prasad,*[,†] Jawad Naciri,[‡] and B.R. Ratna[‡]

[†]Centre for Soft Matter Research, Jalahalli, Bangalore 560 013, India

[‡]Naval Research Laboratory, Center of Bio/Molecular Science and Engineering, 4555 Overlook Avenue, Washington D.C. 20375, United States

ABSTRACT: In contrast to the exhaustive measurements of various properties of ferroelectric liquid crystals at atmospheric pressure, only a few studies exist at high pressure. Here we report the isobaric thermal variation of spontaneous polarization (P_s), coercive voltage (U_{xc}), and rotational viscosity (γ_ϕ) of a ferroelectric liquid crystal (10PPBN4) as a function of applied pressure. The material having a high value of P_s exhibits a trend reversal: as the temperature is lowered below the transition from the smectic A to the smectic C* (ferroelectric) phase, P_s increases to begin with but after reaching a maximum decreases with further decrease in temperature. Interestingly, the trend reversal feature becomes more dominant as the pressure is increased. Further, at a fixed reduced temperature with respect to the transition, all three parameters P_s, U_{xc}, and γ_ϕ decrease with pressure. We show that the data can be well described by a model developed for materials exhibiting a sign reversal in P_s. The single characteristic parameter of the model, viz., the ratio of the inversion temperature (at which P_s changes sign), to the transition temperature, is seen to increase with pressure, corroborating predominance of trend reversal at elevated pressures observed experimentally.

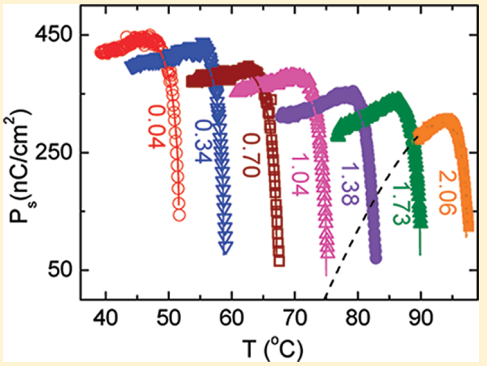

1. INTRODUCTION

The liquid crystalline smectic (Sm) phases show a layer structure in addition to the orientational order common to all liquid crystal (LC) phases. In the smectic A (A) phase, the director (representing the average orientation direction of the molecules) is parallel to the layer normal, while in the smectic C (C) phase they are tilted with respect to it. However, the arrangement of the molecules within the layer is liquid-like in both cases. The chiral versions of these two smectics, labeled SmA* (or sometimes simply SmA) and SmC*, exhibit certain interesting properties and have attracted much attention.[1] In the nonchiral SmA and SmC phases, the symmetry is so high that free rotation around the long molecular axis and head-to-tail invariance prevent the occurrence of ferroelectricity. In the SmC* phase, however, the absence of mirror planes leads to the appearance of spontaneous polarization in a direction which is perpendicular to the plane containing the layer normal and the tilted molecule. However, the presence of chirality induces a slight precession of tilt direction from layer to layer and hence in the in-plane polarization. This results in the formation of a helical structure with its axis parallel to the layer normal averaging out the net polarization to zero. The helix can be unwound by the application of either external fields or surface forces, leading to a finite polarization. Phase transitions involving these ferroelectric liquid crystals (FLCs) have been of significant interest, owing to the presence of multiple order parameters, coupling between them, etc.

Although the first high-pressure experiments[2] were carried out soon after the discovery of LC, only much later the field has become active. These high-pressure studies providing valuable insight into the behavior of LC materials have much concentrated on the nematic and smectic A phases [see review articles[3−6]]. On the other hand, the physical properties of FLCs have been studied quite exhaustively at atmospheric pressure,[7] but only a few reports concerning the effect of applied pressure are available.[8] The reason for this could be the type of challenges one faces in the design of the experimental setup. For electrical investigations of liquid crystals, certain factors not encountered in the high-pressure study of the solid state have to be taken into account, for example, the containment of the fluid samples in the high-pressure cell, the possibility of chemical reactivity with the pressure transmitting media, small dielectric constant, and electric polarization, etc. In this article, we describe the dependence of spontaneous polarization, coercive voltage, and rotational viscosity of a FLC compound on both temperature and applied pressure. Comparisons are made concerning the behavior of polarization with temperature at various pressures with the predictions of a theoretical model.

2. EXPERIMENTAL SECTION

The molecular structure and the phase sequence of the compound used, 10PPBN4, are given in Figure 1. The high-pressure setup employed is a modified form of the optical cell[9] and is similar to the one used for dielectric measurements.[10] Essentially it consists of the sample contained in a PET gasket (thickness ~0.06 mm) sandwiched between two steel cylinders, which also

Received: April 29, 2011
Revised: June 13, 2011
Published: August 02, 2011

dx.doi.org/10.1021/jp203979z | *J. Phys. Chem. B* 2011, 115, 10425–10430

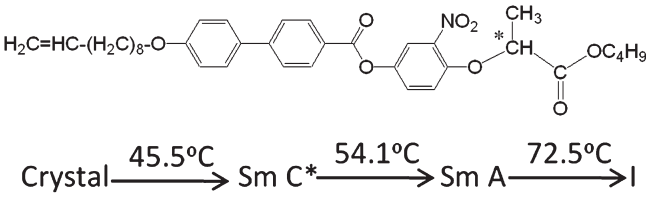

Figure 1. Molecular structure and transition temperatures of the studied compound, 10PPBN4. The labels SmC*, SmA, and I stand for smectic C*, smectic A, and isotropic phase, respectively.

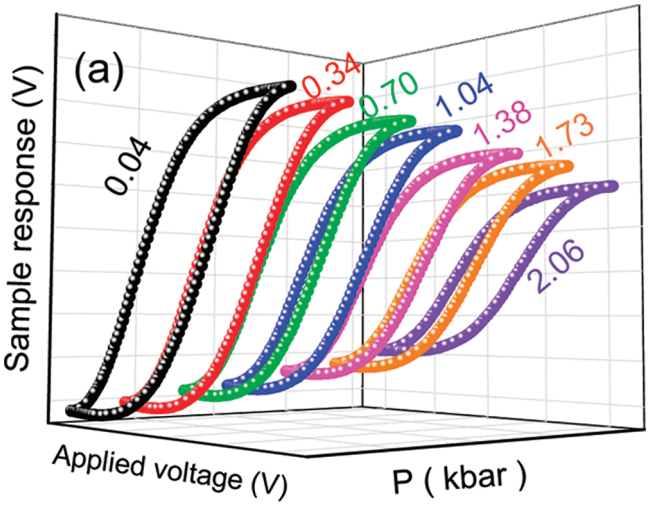

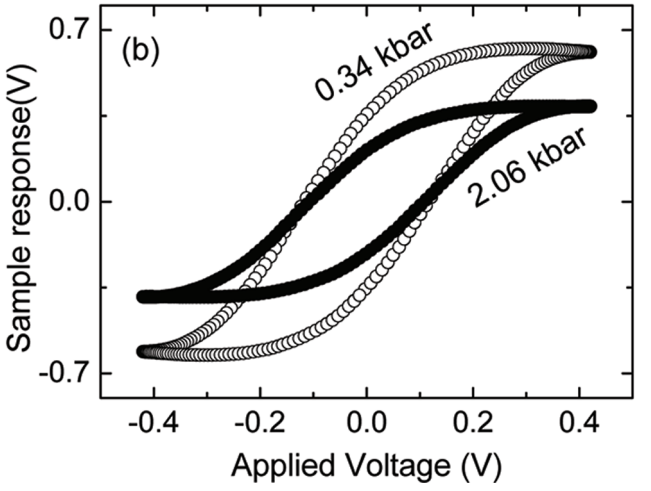

Figure 2. (a) Illustration of the pressure dependence on the polarization hysteresis curves at a fixed relative temperature of $T_{SmA\text{-}SmC^*}$-10 °C, where $T_{SmA\text{-}SmC^*}$ is the transition temperature at each pressure. Notice the significant reduction in the height of the loops with pressure indicating diminution of the magnitude of P_s. The number given against each loop indicates the applied pressure. (b) 2D representation of the data in (a) at two different pressures, to highlight the change in the loop characteristics with pressure.

serve as electrodes, and enclosed in an elastomer tube. The elastomer tube also serves to prevent contamination of the sample by the pressure-transmitting fluid (Plexol). Care was taken to make

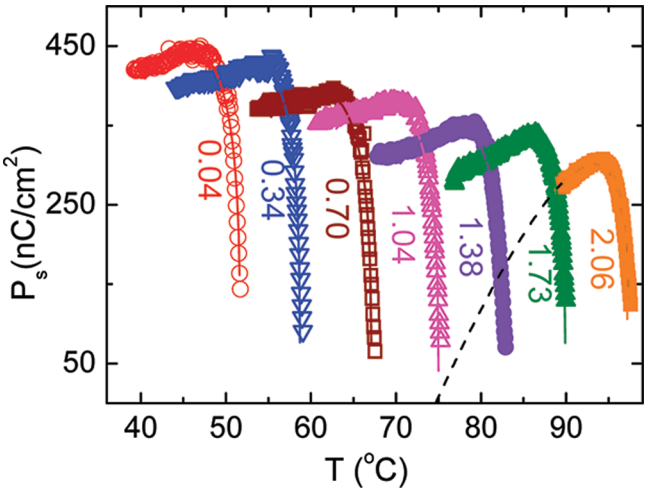

Figure 3. Temperature dependence of the spontaneous polarization at several pressures. At all pressures, on cooling the sample below the SmA−SmC* transition, P_s exhibits a sharp rise and a trend reversal after reaching a maximum, a feature that becomes prominent at higher pressures. The solid lines represent fitting to eq 3. The possibility of reaching the T_{inv} point as determined from eq 3 is shown as a dashed line for the highest pressure data set.

sure that the sample assembly was electrically isolated from the rest of the high-pressure setup. The surfaces of the steel cylinders in contact with the sample were pretreated with a polyimide layer to promote planar alignment of the LC molecules. Screws threaded into the steel cylinders established electrical contact between the sample and the measuring equipment. The sample temperature was sensed by a K-type thermocouple and measured using a digital multimeter (Keithley DMM 2000) to a precision of ±10 mK. In this setup, the sample pressure is the same as that in the plumbing line and thus could be conveniently measured with a high-precision (±3 bar) Heise gauge.

The polarization measurements were made using a standard Diamant bridge setup.[11] The electrical switching of the sample was achieved by applying a sinusoidal field to the sample using a function generator (Agilent 33220A) whose output was amplified with a high voltage power supply (TREK, model 50/75). The outputs from the sample arm and the compensating arm of the bridge were fed to the inputs of a pin-programmable-gain difference amplifier (Analog Devices, AD 524) to produce a balanced hysteresis loop. The applied waveform and the output waveform of the difference amplifier were fed to two different channels of a digital oscilloscope (Agilent DSO5054A). The oscilloscope and the temperature measuring DMM were interfaced to a PC through the IEEE 488 bus, which enabled the data acquisition process to be automated by a user-written program. Measurements were conducted along isobars; i.e., the temperature was swept by keeping the pressure constant.

3. RESULTS AND DISCUSSION

3.1. Spontaneous Polarization. The polarization hysteresis curves obtained at a relative temperature of $T_{SmA\text{-}SmC^*}$-10 °C for a number of pressures are shown in Figure 2a; the data for two representative pressures are shown in Figure 2b, in a 2D representation for ease of comparison. In these profiles, a feature that stands out is that with increasing pressure the height of the

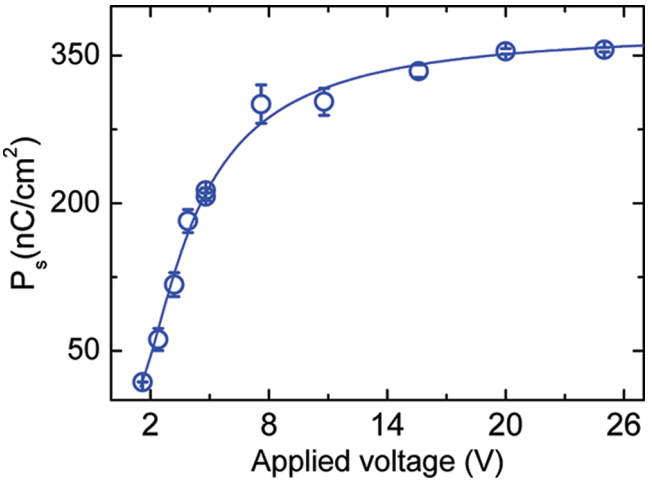

Figure 4. Dependence of P_s on applied voltage at atmospheric pressure. To be noted is the fact that P_s has a sharp increase at low voltages and a gentle one at higher voltages. The solid is only a guide to the eye.

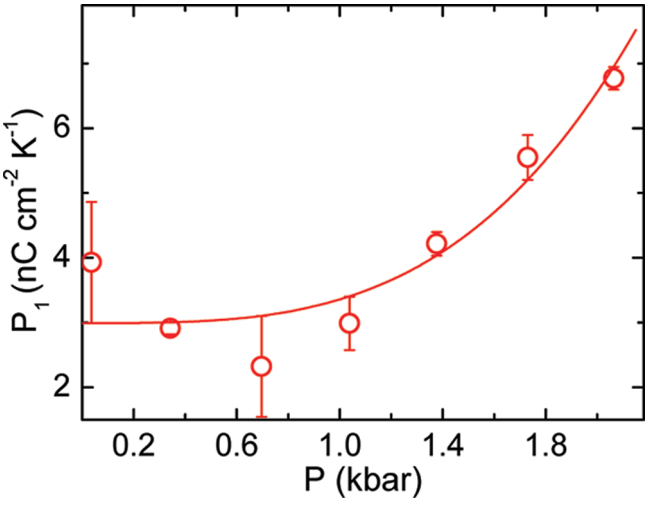

Figure 5. Pressure dependence of the slope P_1 extracted from fitting the P_s data to eq 1, suggesting that the trend reversal becomes substantial at higher pressures. The line serves as a guide to the eye.

loop, which is a measure of the sample polarization, decreases substantially. Notice that the coercive field (E_c) as well as the field necessary for polarization saturation (P_s) are influenced to a much smaller extent.[1,12] The temperature dependence of polarization at several pressures is displayed in Figure 3. [A remark that should be made at this point is that a thicker sample, than usually employed for ferroelectric samples, is unavoidable in our high-pressure setup. To account for the presence of the spacer in the active area, we compared the data at the lowest pressure with those obtained at atmospheric pressure using glass cells. The good agreement found between the two sets indicates that the alignment of the sample in the high-pressure cell is of good quality.] At each pressure as the temperature is lowered below $T_{SmA\text{-}SmC^*}$ the polarization increases precipitously to begin with, reaches a maximum, and then decreases. The latter behavior becomes more conspicuous at higher pressures. The existence of such a feature as well as the value of the polarization, well away from the SmA−SmC* transition, are at variance with an earlier

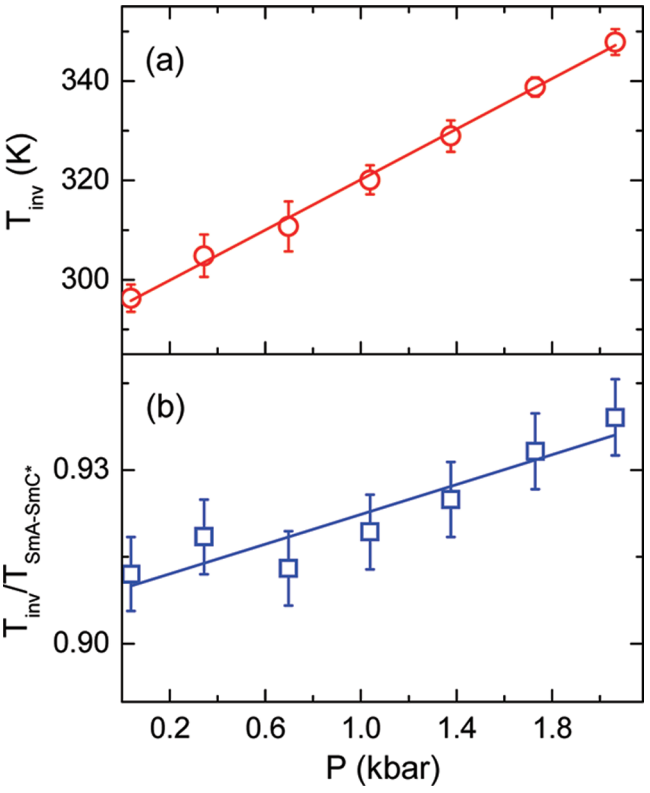

Figure 6. Plot exhibiting (a) absolute value of the inverse temperature T_{inv} and (b) its ratio to the transition temperature $T_{SmA\text{-}SmC^*}$ varying linearly with pressure, with the solid line representing the best fit to a straight line in both cases.

report by the Washington group.[13] It must be mentioned here that the earlier study employed the triangular wave method to measure the polarization and also had used a much higher (12 V/μm) field. Unlike the hysteresis loop method, the drawback of the triangular wave method is that it is not possible to determine whether the applied field is sufficient or much higher than the one required to unwind the helix of the SmC* phase. The assumption in these measurements is that once the helix is unwound further increase in the field does not alter the polarization much. To find out whether this is true for the present sample also, we determined the polarization as a function of the magnitude of the field. As seen in Figure 4, at atmospheric pressure for a temperature of 42 °C, in region I immediately above zero field the polarization increases rapidly as the field is increased and then in region II changes slope revealing a gradual variation. Although the field dependence of polarization is much smaller in region II, it is substantial. Making a simple assumption that the variation is linear, the slope turns out to be 3.7 nC cm^{-2}V^{-1}. The hysteresis loop (Figure 2) shows that the E_s (field required to obtain saturation polarization) value is 1 V/μm, whereas the earlier work had employed an order of magnitude higher field. Using the slope value mentioned above, we arrive at the polarization value of ~600 nC/cm^2 reported in ref 13. This indicates that field-induced polarization is quite large for this material, and with high fields the total polarization obtained can be substantially larger than the spontaneous value. In the present study, we have employed fields just enough to realize the spontaneous polarization, and therefore the field-induced values can be considered to be at a minimum. Comparing the present results with the earlier

Table I. Parameters Extracted from the Best Fit of the Data to Equation 3 at Various Pressures

P (kbar)	m	T_{inv} (K)	P_{so} (nC/cm^2)	$T_{SmA\text{-}SmC^*}$ (K)
2.06	0.21 ± 0.03	347.8 ± 2.6	12.2 ± 1.5	370.36 ± 0.03
1.73	0.26 ± 0.02	338.8 ± 1.9	11.5 ± 0.9	363.04 ± 0.02
1.38	0.27 ± 0.03	328.9 ± 3.1	10.4 ± 1.2	355.60 ± 0.04
1.04	0.30 ± 0.03	320.1 ± 2.9	10.1 ± 1.0	348.15 ± 0.04
0.70	0.28 ± 0.04	310.7 ± 5.0	10.2 ± 1.7	340.26 ± 0.04
0.34	0.27 ± 0.03	304.8 ± 4.3	12.8 ± 2.1	331.85 ± 0.03
0.04	0.27 ± 0.02	296.2 ± 2.7	12.2 ± 1.2	324.81 ± 0.03

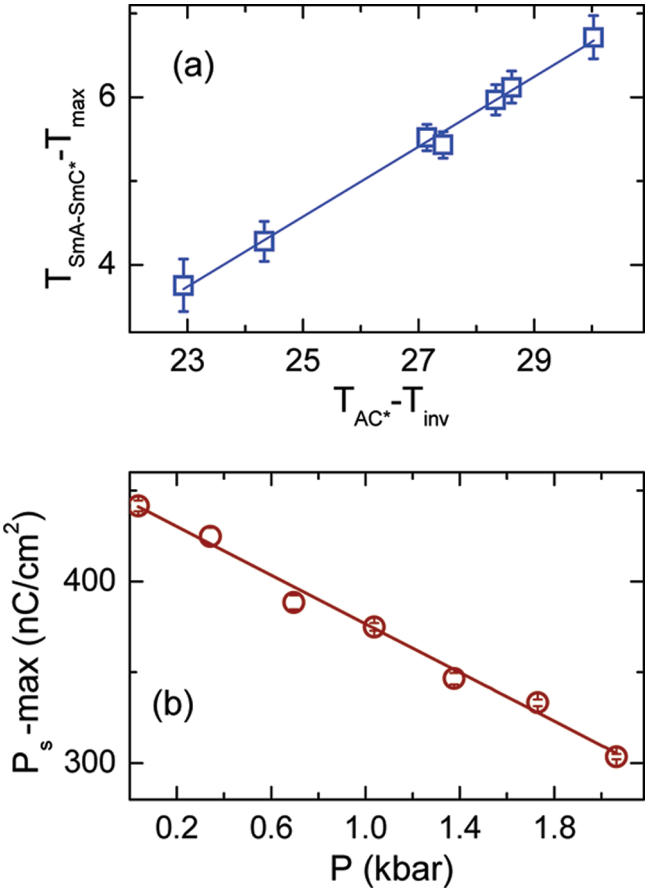

Figure 7. Diagram to show the validity of the temperatures T_{max} and T_{inv} taken relative to the transition temperature. The linear relation between the two parameters is shown as a solid line. (b) Influence of pressure on the maximum value of polarization, which is given by the value of P_s at T_{max}. P_s-max is seen to be linearly decreasing with pressure, as indicated by the straight line fit (solid line).

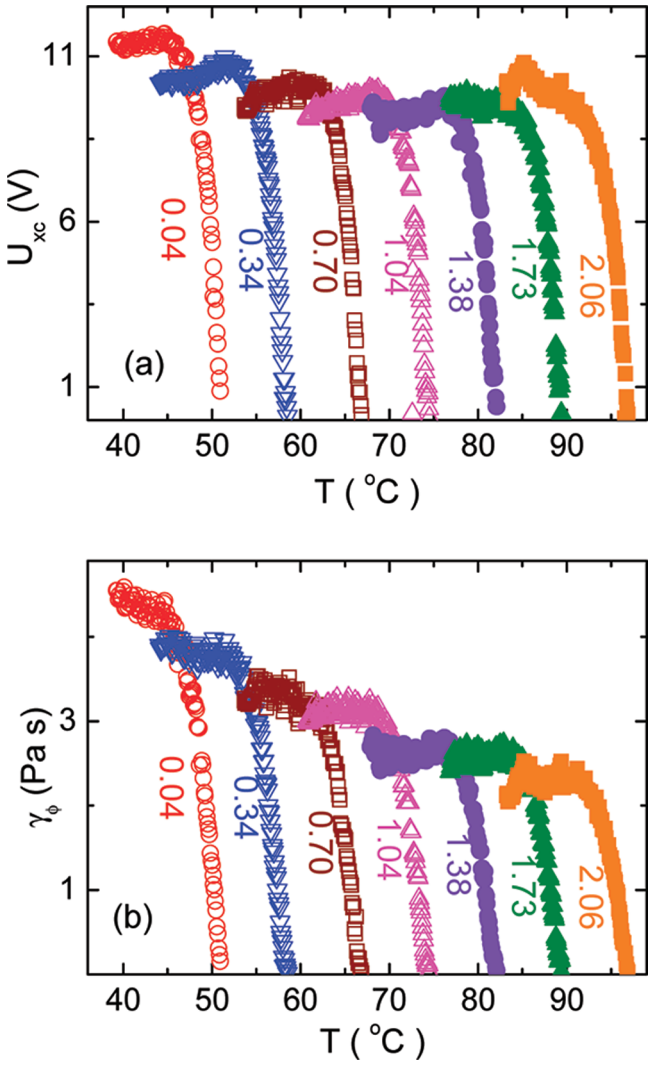

Figure 8. Thermal variation of (a) the coercive voltage U_{xc} and (b) the rotation viscosity at several pressures, whose values are indicated against each data set. A slight nonmonotonic variation of the former and a substantial decrease of the latter are observed as the pressure is increased.

work, we conclude that in this compound the actual temperature dependence of polarization can depend on whether the field-dependent polarization is high or not. Whereas the total polarization[13] exhibits only a monotonic increase with decreasing temperature, the spontaneous polarization P_s (Figure 3) displays that after reaching a maximum, the value starts decreasing.

We first analyze the data only at temperatures lower than the one where P_s reaches a maximum. The trend with temperature suggests a linear variation, and therefore we fit this part of the data to a linear equation

$$P_s(T) = P_o + P_1 T \quad (1)$$

Figure 5 shows that the slope, P_1, is hardly dependent on pressure up to 1 kbar and then a large increase with pressure, suggesting that the trend reversal becomes more dominant at higher pressures.

The trend reversing with temperature observed here is in a sense similar to the case of polarization reversal materials: after reaching a maximum, P_s decreases with temperature completely vanishing at an *inversion temperature* (T_{inv}), below which it grows again monotonically but with the opposite sign.[14,15] This phenomenon has been interpreted in different ways. Glass et al.[16] ascribe it to competing molecular conformations which produce opposite contributions to P_s. In another viewpoint, the competing effects arise from the polar and quadrupolar biasing of rotations around the long molecular axis.[17] More recently, Photinos and his collaborators[15] have analyzed this problem on the basis that the symmetries and the conformational structure of the real molecules give rise to several, mutually independent, tilt order

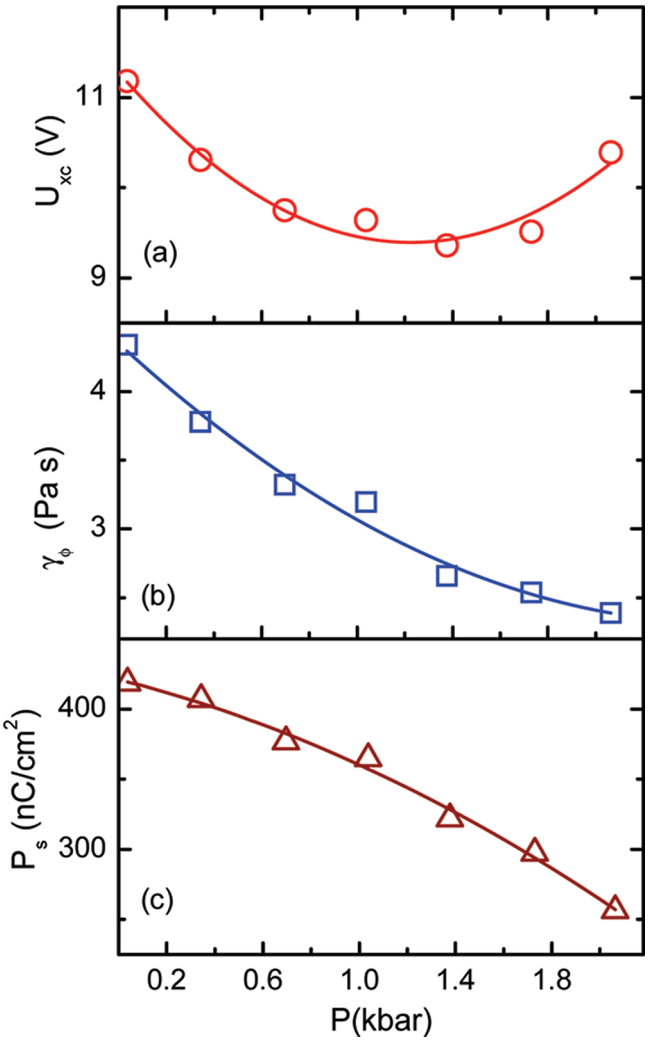

Figure 9. Variation with pressure of (a) the coercive voltage, (b) rotational viscosity, and (c) polarization at a fixed relative temperature of $T_{SmA\text{-}SmC^*}$-10, bringing out in clear terms the sole influence of pressure, qualitatively seen in Figures 3 and 8. The solid lines merely serve to show the tendencies.

parameters and also to polar arrangement of the molecules. This has been modeled in terms of two (as against the conventionally used single) tilt order parameters, labeled primary and secondary, and an indigenous polarity order parameter P_I. From the viewpoint of a Landau free-energy expansion, this required inclusion of a higher-order piezoelectric polarization−tilt coupling term. The analysis yielded the following expression for the thermal variation of P_s

$$P_s \sim (T - T_{inv})\sqrt{T_{SmA-SmC^*} - T} \quad (2)$$

This equation however has an implicit assumption that the tilt angle varies as the square root of the temperature reduced with respect to the SmA−SmC* transition temperature. Since the temperature dependence of the tilt angle is not known for the present case and also to account for a more general situation, we relax this condition and write

$$P_s = P_{so}(T - T_{inv})(T_{SmA-SmC^*} - T)^m \quad (3)$$

Here P_{so} and m are amplitude and exponents containing the temperature dependence of the tilt angle in an implicit form. (It may be noted that even in the P_s-sign-inversion materials the tilt angle varies monotonically with temperature.) The data in Figure 3 have been analyzed using eq 3, and the fitting is quite satisfactory. Interestingly, the extracted T_{inv} values are seen to increase linearly with increasing pressure (see Table I, Figure 6a) with a slope of 25.4 ± 0.5 K/kbar. According to the analysis by Karahaliou,[15] a single characteristic reduced temperature $R = T_{inv}/T_{SmA\text{-}SmC^*}$ determines the thermal behaviors of the polarity order parameter P_I and of the spontaneous polarization, varying from the commonly observed monotonic variation to the sign-inverting type. Obviously, if $R > 1$ ($T_{inv} > T_{SmA\text{-}SmC^*}$), a strictly monotonic increase of P_s with temperature is observed. On the other hand, for $R < 1$ ($T_{inv} < T_{SmA\text{-}SmC^*}$), the realization of inverting behavior depends on the stability of the SmC* phase also. From Table I and Figure 6b, it is seen that at all the pressures studied the compound used here shows a value closer to but, importantly, smaller than 1. Thus, the observation of a local maximum followed by a decrease in P_s as the temperature is lowered is in line with the theoretical analysis and gives credence to our analysis. The fact that the value of $T_{inv}/T_{SmA\text{-}SmC^*}$ increases with pressure points to the maximum in P_s occurring closer to the SmA−SmC* transition, as indeed seen experimentally. These features suggest that if the observed effects are due to different conformers pressure tends toward stabilizing a single conformer.

The theoretical analysis also predicts the temperature at which P_s reaches a maximum to be dependent on the difference between $T_{SmA\text{-}SmC^*}$ and T_{inv}. This is borne out to be true in the experiments (Figure 7(a)), with a small change that the variation is between the relative temperatures given by

$$T_{SmA-SmC^*} - T_{max} \sim T_{SmA-SmC^*} - T_{inv} \quad (4)$$

Concomitant with the increase in T_{max}, the maximum value of P_s decreases as the pressure is increased (Figure 7b).

3.2. Coercive Voltage and Rotational Viscosity. The polarization hysteresis loops can be used to extract values of the coercive voltage as well as the rotational viscosity associated with the ferroelectric switching. For the latter parameter, we have employed the following expression suggested by Escher et al.[18]

$$\gamma_\phi = \frac{C(U_y^s)^2 U_{xc}}{Ad\omega\left(\frac{dU_y}{dU_x}\right)_c \sqrt{U_o^2 - U_{xc}^2}} \quad (5)$$

Here U_y^s is the maximum value of the sample response; $U_x = U_o \sin \omega t$ is the applied voltage having a frequency ω; U_{xc} is the value of the applied voltage at the zero-crossing point c; C is the standard capacitance of the bridge circuit; and A and d are the area and thickness of the sample. Figures 8(a) and (b) present the temperature dependence of U_{xc} and γ_ϕ for various pressures, showing behaviors similar to that of P_s. To look at the effect of pressure alone, the values at a fixed reduced temperature of $T_{SmA\text{-}SmC^*}$-10 °C are given as a function of pressure in Figures 9(a) and (b), respectively. For comparison, the P_s values at the same reduced temperature are shown in panel (c). All the parameters show a general decrease with increasing pressure, although U_{xc} exhibits a slight increase after having a minimum. A general observation on smectic systems is that the stability of the SmC (or SmC*) phase diminishes with increasing pressure.[19] This does not appear to be the case in the case of 10PPBN4 studied here, as the pressure−temperature phase diagram (Figure 10),

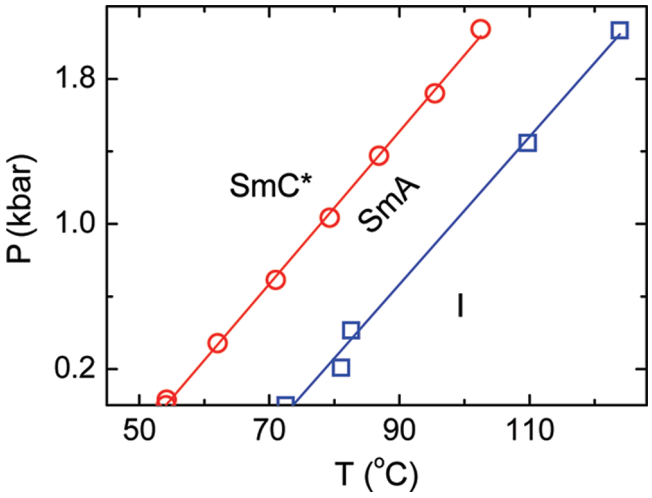

Figure 10. Pressure−temperature phase diagram presenting the linear dependence of the I−SmA and SmA−SmC* phase boundaries.

determined using low-frequency dielectric constant data, shows a clearly seen SmA−SmC* phase line right up to the highest pressure studied. A definite possibility is that the magnitude of the tilt angle decreases with increasing pressure, owing to which the three parameters (P_s, U_{xc}, and γ_ϕ) also decrease. However, an X-ray study conducted[20] on a different material (very few measurements of tilt angle at high pressure exist in the literature) suggests that the maximum tilt achieved is hardly affected by pressure. A third possibility is that the polarization−tilt coupling diminishes with increasing pressure causing the values of all three parameters to diminish. Tilt angle measurements at high pressure for the studied material are required to check this feature.

SUMMARY

We have performed detailed investigations of the spontaneous polarization, coercive field, and rotational viscosity of a ferroelectric liquid crystal as a function of both temperature and pressure. The most salient feature of the study is the observation of the trend reversal in polarization as a function of temperature at all pressures, with the effect becoming increasingly dominant at elevated pressures. Predictions made by a model proposed for materials exhibiting a sign reversal in polarization have been found to describe these observations quite well.

AUTHOR INFORMATION

Corresponding Author

*E-mail: skpras@gmail.com.

REFERENCES

(1) Lagerwall, S. T. *Ferroelectric and Antiferroelectric Liquid Crystals*; John Wiley & Sons: New York, 1999.

(2) Hulett, G. A. *Z. Phys. Chem.* **1899**, *28*, 629–672.

(3) Chandrasekhar, S.; Shashidhar, R. In *Advances in Liquid Crystals*; Brown, G. H., Ed.;Academic Press: London, 1979; Vol. 4.

(4) Urban, S.; Wurlfinger, A. *Adv. Chem. Phys.* **1997**, *93*, 143–216.

(5) Pollmann, P. In *Physical properties of liquid crystals*; Demus, D., Goodby, J., Gray, G. W., Spiess, H. W., Vill, V., Eds.; Wiley VCH: Weinheim, 1999.

(6) Krishna Prasad, S. Liquid crystals under high pressure. In *The Encyclopedia of Materials: Science and Technology*; Buschow, K. H. J. et al. , Eds.; Elsevier Science Ltd.: Amsterdam, 2001.

(7) For reviews see: Musevic, I.; Blinc, R.; Zeks, B. *The Physics of Ferroelectric and Antiferroelectric Liquid Crystals*; World Scientific: Singapore, 2000.

(8) Yasuda, N.; Fujimoto, S.; Funa, S. *J. Phys. D: Appl. Phys.* **1985**, *18*, 521–530. Uehara, H.; Hatano, J. *Jpn. J. Appl. Phys.* **2007**, *46*, 7125–7127. Uehara, H.; Hatano, J. *Ferroelectrics* **2007**, *355*, 154–158. Uehara, H. *Jpn. J. Appl. Phys.* **2008**, *47*, 7635–7637. Khened, S. M.; Krishna Prasad, S.; Raja, V. N.; Chandrasekhar, S.; Shivkumar, S. *Ferroelectrics* **1991**, *121*, 307–318. Krishna Prasad, S.; Khened, S. M.; Chandrasekhar, S. *Ferroelectrics* **1993**, *147*, 351–365. Nair, G. G.; Krishna Prasad, S.; Chandrasekhar, S. *Mol. Cryst. Liq. Cryst.* **1995**, *263*, 311–323. Shankar Rao, D. S.; Krishna Prasad, S.; Chandrasekhar, S.; Mery, S.; Shashidhar, R. *Mol. Cryst. Liq. Cryst.* **1997**, *292*, 301–310.Prasad, S. K.; Khened, S. M.; Chandrasekhar, S. In *Modern Topics in Liquid Crystals; From neutron scattering to ferroelectricity*; Buka, A., Ed.; World Scientific: Singapore, 1994; pp 285−299.

(9) Krishna Prasad, S.; Shankar Rao, D. S.; Jeyagopal, P. *Phys. Rev. E* **2001**, *64*, 011706-1–4.

(10) See, e.g: Bapat, P. N.; Shankar Rao, D. S.; Krishna Prasad, S.; Yelamaggad, C. V. *J. Phys. Chem. B* **2010**, *114*, 12825–12832.

(11) Diamant, H.; Drenck, K.; Pepinsky, R. *Rev. Sci. Instrum.* **1957**, *28*, 30–33.

(12) Strictly speaking, for a ferroelectric liquid crystal with a helical structure, there is no coercive force, but we follow the similarity with the solid ferroelectrics and define the coercive field as the field seen at the zero-crossing point of the hysteresis loop.

(13) Naciri, J.; Ratna, B. R.; Baral-Tosh, S.; Keller, P.; Shashidhar, R. *Macromolecules* **1995**, *28*, 5274–5279.

(14) Goodby, J. W.; Chin, E.; Geary, G. M.; Patel, J. S.; Finn, P. L. *J. Chem. Soc., Faraday Trans. 1* **1987**, *83*, 3429–3446. Yoshino, K.; Ozaki, M.; Nakao, K.; Taniguchi, H.; Yamasaki, N.; Satoh, K. *Liq. Cryst.* **1989**, *5*, 1213–1218. Saito, S.; Murashiro, K.; Kikuchi, M.; Inukai, T.; Demus, D.; Neudorf, M.; Diele, S. *Ferroelectrics* **1993**, *147*, 367–394. Eidenschink, R.; Geelhaar, T.; Andersson, G.; Dalhgren, A.; Flatischler, K.; Gouda, F.; Lagerwall, S. T.; Skarp, K. *Ferroelectrics* **1988**, *84*, 167–181.

(15) Karahaliou, P. K.; Vanakaras, A. G.; Photinos, D. J. *Phys. Rev. E* **2002**, *65*, 031712–1−13.

(16) Glass, A. M.; Goodby, J. W.; Olson, D. H.; Patel, J. S. *Phys. Rev. A* **1988**, *38*, 1673–1675.

(17) Kuntjak-Urbanc, B.; Zeks, B. *Liq. Cryst* **1995**, *18*, 483–488. In fact, the behavior observed in the present study, viz., there is a trend reversal but not sign reversal of the thermal variation of P_s, is referred to as the non-monotonic type by these authors.

(18) Escher, C.; Dubal, H. R.; Hemmerling, W.; Miller, I.; Ohlendorf, D.; Wingen, R. *Ferroelectrics* **1988**, *84*, 89–101.

(19) Shashidhar, R.; Chandrasekhar, S. *Mol. Cryst. Liq. Cryst.* **1983**, *99*, 297–300. Kalkura, A. N.; Shashidhar, R.; Venkatesh, G.; Neubert, M. E.; Ferrato, J. P. *Mol. Cryst. Liq. Cryst.* **1983**, *99*, 177–183. Krishna Prasad, S.; Ratna, B. R.; Shashidhar, R.; Surendranath, V. *Ferroelectrics* **1984**, *58*, 101–105.

(20) Guillon, D.; Stamatoff, J.; Cladis, P. E. *J. Chem. Phys.* **1982**, *76*, 2056–2063.